Alumina-Promoted Sulfated Zirconia System: Structure and Microstructure Characterization

Patrizia Canton,[†] Roberta Olindo,[‡] Francesco Pinna,*[,‡] Giorgio Strukul,[‡] Pietro Riello,[†] Moreno Meneghetti,[§] Giuseppina Cerrato,[||] Claudio Morterra,[||] and Alvise Benedetti[†]

Dipartimenti di Chimica Fisica and Chimica, Università Ca'Foscari di Venezia, 30123 Venezia, Italy, Dipartimento di Chimica Fisica, Università di Padova, 35122 Padova, Italy, and Dipartimento di Chimica IMF, Università di Torino, 10125 Torino, Italy

Received June 6, 2000. Revised Manuscript Received October 19, 2000

The Al_2O_3 promotion of ZrO_2/SO_4 has been shown to influence *n*-butane isomerization activity. In this paper we report a study of the influence of a small addition of Al_2O_3 (0.6−10.3 wt %) onto the ZrO_2 structure and microstructure. The addition of alumina is related to an increase of the surface area. A detailed X-ray diffraction analysis by the use of the modified Rietveld method allowed us to follow the changes in the crystalline phases and to quantify the amount of amorphous phase. When the Al_2O_3 content is increased, a decrease of the ZrO_2 particle sizes is observed, paralleled by an increase of the amorphous phase. When the Al_2O_3 content is larger than 3.7 wt %, only amorphous phase can be detected. No crystalline peaks of Al_2O_3 were ever observed. These data were supported also by TEM and Raman measurements.

1. Introduction

Sulfated zirconia (ZrO_2/SO_4) has been the subject of extensive research work since its ability to catalyze the isomerization of linear to branched light hydrocarbons was first discovered.[1]

ZrO_2/SO_4 is usually prepared by sulfation of an amorphous zirconium hydroxide precursor, followed by calcination treatment. The properties of the resultant ZrO_2/SO_4 system strongly depend on the preparation procedures, that is, on the nature of the starting material, sulfation method, sulfur content, calcination temperature, and so forth.[2,3]

Unfortunately, rapid deactivation of the catalyst is always observed. The addition of small amounts of promoters, like for instance Pt,[4] Fe and Mn,[5] and Ni,[6] was found to increase the activity in the isomerization of *n*-butane, although only in the case of Pt a catalyst with good stability was obtained.

Gao et al.[7] recently reported that the addition of small amounts of Al_2O_3 to the ZrO_2/SO_4 system leads to catalysts that are both more active than the corresponding nonpromoted sulfated zirconia and, more interesting, very stable with reaction time if the *n*-butane isomerization reaction is performed at 523 K in the presence of H_2. According to the authors, the remarkable activity and stability of the Al-promoted catalysts are due to a different distribution of acid sites strength and to an enhanced number of acid sites with intermediate strength. However, little attention was paid by the authors to the structural characterization of the $ZrO_2-Al_2O_3$ system.

At the same time, other studies have been reported that are concerned with the preparation and the morphological characterization of sulfated zirconia supported on alumina or silica,[8,9] all with the aim of obtaining a zirconia-based catalyst with high specific surface area.

Recently, Zalewsky et al.[10] reported the characterization of catalytically active sulfated zirconia systems containing silica or alumina. The incorporation of these oxides into the catalytic system has been claimed to limit the formation of large zirconia crystallites, with consequent stabilization of the tetragonal crystal phase for samples containing about 20 wt % of alumina.

The reported results underline the fact that alumina can greatly affect the chemical and structural properties of the ZrO_2 modifying the final oxide phase. However, the above papers are mostly focused on the catalytic properties of the systems. They do not report a detailed analysis of the influence of different amounts of Al_2O_3 on the ZrO_2 structure, especially when very low amounts

* To whom correspondence should be addressed: Dipartimento di Chimica, Università Ca'Foscari di Venezia, Dorsoduro 2137, 30123 Venezia, Italy. E-mail: pinna@unive.it. Fax: +39-041 257 8517.
[†] Dipartimento Chimica Fisica, Università Ca'Foscari di Venezia.
[‡] Dipartimento di Chimica, Università Ca'Foscari di Venezia.
[§] Università di Padova.
[||] Università di Torino.

(1) Hino, M.; Kobayashi, S.; Arata, K. *J. Am. Chem. Soc.* **1979**, *101*, 6439.
(2) Corma, A. *Chem. Rev.* **1995**, *95*, 559.
(3) Song, X.; Sayari, A. *Catal. Rev.-Sci. Eng.* **1996**, *38*, 329.
(4) Ebitani, K.; Knoishi, J.; Hattori, H. *J. Catal.* **1991**, *130*, 257.
(5) Holstein, E. J.; Wei, J. T.; Hsu, C.-Y. U.S. Patent 4918041, 1990.
(6) Coelho, M. A.; Resasco, D. E.; Skabwe, E. C.; White, R. L. *Catal. Lett.* **1995**, *32*, 256.
(7) Gao, Z.; Xia, Y.; Hua, W.; Miao, C. *Top. Catal.* **1998**, *6*, 101.
(8) Huang, Y.; Zhao, B.; Xie, Y. *Appl. Catal. A* **1998**, *73*, 27.
(9) Chuah, G. K. *Catal. Today* **1999**, *49*, 131.
(10) Zalewski, D. J.; Alerasool, S.; Doolin, P. K. *Catal. Today* **1999,** *53*, 419.

10.1021/cm001101z CCC: $20.00
Published on Web 04/05/2001

of alumina are added and when it is possible to follow the continuous, albeit small, modifications of the parent structure of ZrO_2.

In the present paper we report a study of the influence of alumina on the ZrO_2 structure in the range (0−10 wt %) to follow in detail the structural and microstructural evolution of the ZrO_2 phases (amorphous or crystalline).

2. Experimental Section

2.1. Samples Preparation. Samples were prepared via a conventional precipitation method. $ZrOCl_2 \cdot 8H_2O$ (Fluka, >98%) and the required amount of $Al(NO_3)_3 \cdot 9H_2O$ (Aldrich, 98%) were dissolved in distilled water and added dropwise under vigorous mechanical stirring to a 10 N ammonia solution. During the entire course of precipitation the pH value was kept constant at 8 by simultaneous addition of aqueous ammonia. After the complete addition of the two salt solutions, the hydroxide suspension was stirred for 30 min and aged for 15 h at room temperature. The aged precipitate was filtered and thoroughly washed with distilled H_2O until the disappearance of chloride ions ($AgNO_3$ test). The precipitate was then dried at 383 K for 20 h and powdered to below 50 mesh. Sulfation was carried out by incipient wetness impregnation of the zirconium hydroxide with an aqueous $(NH_4)_2SO_4$ solution. The sulfated samples were dried again at 383 K for about 20 h, then calcined at 923 K for 3 h under dry air (30 mL/min), and stored in air.

As reference systems, plain ZrO_2/SO_4 (ZS) and Al_2O_3/SO_4 (AS) were prepared in a similar way starting from $ZrOCl_2 \cdot 8H_2O$ and $Al(NO_3)_3 \cdot 9H_2O$ solutions, respectively.

The alumina-promoted catalysts are hereafter labeled as ZSA*x*, with *x* corresponding to the nominal alumina concentration (% mol).

2.2. Characterization Techniques. 2.2.1. Analytical Data. The quantitative determination of sulfates was performed by ion chromatography.[11] The powdered sample was suspended in 0.1 M NaOH and filtered through a 0.5-μm PTFE filter. The apparatus consisted of a model LC20 ion chromatograph (Dionex Corp., USA). The analytical columns were of the anion-exchange type: a guard column (Dionex AG 14, 50 × 4 mm id) and a separator column (Dionex AS 14, 250 × 4 mm id). Detection was achieved by a micromembrane suppressor (ASRS-II) and a conductivity detector. The eluent was a carbonate−hydrogen carbonate buffer. All sulfate concentrations were calculated as the average of two independent sample treatments.

The quantitative determination of Al was performed by atomic absorption spectrometry. The samples were microwave (Milestone mls mega 1200) mineralized in an HF/aqua regia solution.

2.2.2. Textural Properties. The nitrogen adsorption−desorption isotherms were measured at 77 K with a Micromeritics ASAP 2010 system. Prior to measurements, all samples (300 mg) were degassed at 473 K for 3 h. The specific surface areas were calculated according to the BET method; the mesopore size distribution was obtained by the BJH method.[12]

2.2.3. *n*-Butane Isomerization. The catalytic performance of alumina-promoted sulfated zirconia samples was tested in *n*-butane isomerization.[13] The reaction was performed at 523 K and under atmospheric pressure by feeding 25 mL/min of reacting mixture (*n*-butane/H_2 = 1/4) in a fixed-bed reactor. Before reaction the catalyst (0.5 g) was activated in dry airflow at 723 K for 1.5 h. The products analysis was accomplished on-line with a gas chromatograph equipped with TCD.

2.2.4. Acidity Measurements. FTIR spectra were obtained at 2-cm^{-1} resolution with a Bruker IFS88 spectrophotometer. All samples were examined in the form of thin layer deposition (≈5 mg cm^{-2}): powders were first dispersed in water, deposited on a pure Si platelet, and then dried in air at room temperature. The depositions were activated at 673 K in a quartz cell connected to the vacuum line (final $P = 10^{-6}$ Torr) where all adsorption/desorption experiments were also carried out. Pyridine (py) adsorption tests were carried out at room temperature by allowing a large py dose (10 Torr) and then evacuating at the same temperature the excess py after 10 min of contact. All adsorptions were performed in a strictly in situ configuration, which avoids samples contamination and permits spectra ratioing and subtraction.

2.2.5. X-ray Diffraction. The powder diffraction data were collected using a Philips X'Pert vertical goniometer, connected to a highly stabilized generator. Cu Kα Ni-filtered radiation, a graphite monochromator, and a proportional counter with a pulse-height discriminator were used. Data were collected for 10 s with a 0.05° step size on the 10°−140° 2θ range.

Rietveld Method. The Rietveld method has been used to analyze the X-ray data. In general, for a multiphase sample, it is possible to separate the scattering due to the amorphous phase from the scattering belonging to the crystalline phases using a Rietveld analysis with a physically modeled background.[14−16] Once the scattering contributions Y_l have been separated by this fitting procedure, it is possible to assign the weight fractions W_l of each phase, including the amorphous one, by calculating the number of composition units N_l,

$$CN_l = \frac{\int_0^\infty \frac{Y_l}{AP}(s)s^2\,\mathrm{d}s}{\sum_{i=1}^{n_l}\int_0^\infty [|f_i^0|^2 + I_i^{\mathrm{inc}}]s^2\,\mathrm{d}s} \qquad (1)$$

where N_l is the number of composition units (for instance, the molecular unit, composed of *n* atoms) of the *l*th phase, *A* and *P* are the absorption and polarization factor, respectively, f_i^0 is the tabulated atomic scattering factor, I_i^{inc} is the incoherent scattering that can be evaluated using the analytical expression by Smith et al.,[17] $s = 2\sin(\theta)/\lambda$ with 2θ the Bragg angle and λ the radiation wavelength, and *C* is a proportionality constant that is the same for all the phases if no microabsorption effect is present.

This analysis obviously requires the knowledge of the composition of all phases; if this is not known, the problem of finding W_l is also solvable by knowing the global composition of the material and the composition of (M − 1) phases of the M phases constituting the sample. In this case

$$W_l = \frac{N_l \sum_{i=1}^{n_l} w_l^i}{N_G \sum_{i=1}^{n_G} w_l^i} \qquad (2)$$

where N_G is the number of composition units of the whole sample obtained by applying (1) to the global X-ray intensity corrected for the air scattering, n_G is the number of atoms in

(11) Sarzanini, C.; Sacchero, G.; Pinna, F.; Signoretto, M.; Cerrato, G.; Morterra, C. *J. Mater. Chem.* **1995**, *5* (2), 353.
(12) Gregg, S. J.; Sing, K. S. W. *Adsorption; Surface Area and Porosity*, 2nd ed.; Academic Press: London, 1982; p 138.
(13) Olindo, R.; Pinna, F.; Strukul, G.; Canton, P.; Riello, P.; Cerrato, G.; Meligrana, G.; Morterra, C. In *12th International Congress on Catalysis*, Granada, Spain, 2000; Studies in Surface Science and Catalysis 130; Corma, A., Melo, F. V., Mendioroz, S., Fierro, J. L. G., Eds.; Elsevier Science B.V., Amsterdam, 2000; p 2375.
(14) Riello, P.; Fagherazzi; G.; Canton, P. *Acta Crystallogr.* **1998**, *A54*, 219.
(15) Riello, P.; Canton, P.; Fagherazzi, G. *J. Appl. Cryst.* **1998**, *31*, 78.
(16) Riello, P.; Fagherazzi, G.; Clemente, D.; Canton, P. *J. Appl. Crystallogr.* **1995**, *28*, 115.
(17) Smith, V. H.; Thakkar, A. J.; Chapman, D. C. *Acta Crystallogr.* **1975**, *A31*, 391.

Table 1. Analytical and Morphological Data for ZSA*x* Samples

sample	Al_2O_3 (wt %)	BET area (m^2/g)	V_p (cm^3/g)	SO_4 content (wt %)	SO_4 content (groups/nm^2)	L/B ratio
ZS	0.0	84	0.08	3.9	2.9	3.4
ZSA1	0.6	111	0.10	4.1	2.3	3.3
ZSA2	1.2	114	0.11	4.2	2.3	1.8
ZSA3	2.2	113	0.11	6.3	3.5	3.7
ZSA5	3.7	112	0.09	5.0	2.8	2.2
ZSA9	6.0	118	0.10	4.5	2.4	1.5
ZSA15	10.3	128	0.12	5.9	2.9	nd
AS	100.0	192	0.18	5.3	1.7	nd

the composition units, and w_l^i is the atomic weight of the ith of the lth phase.

2.2.6. Raman Spectroscopy. Raman spectra (resolution, 4 cm^{-1}) were recorded at room temperature using a Jobin−Yvon multichannel spectrometer (S3000) equipped with a liquid-nitrogen-cooled CCD camera (Astromed) and the Argon lines of a Coherent Innova 300 Argon−Krypton laser. About 50 mW was focused on an area estimated to be about 200 × 200 μm of a pressed powder sample.

2.2.7. Morphological Properties. (High-resolution) transmission electron microscopy ((HR)TEM) images were obtained with a JEOL JEM 2000-EX instrument, equipped with a top-entry stage and LaB_6 filament and operating at 200-kV acceleration. All powder catalysts were first dispersed in *n*-heptane and then a drop of the suspension was put on a holey carbon Cu grid (200 mesh).

3. Results

Zirconium hydroxide promoted with different amounts of aluminum hydroxide was obtained by coprecipitation at constant pH (8.0) from aqueous solutions of the two salt precursors.

The constant pH value was chosen on the basis of two considerations: (i) to obtain a homogeneous coprecipitation of the two hydroxides because $Al(OH)_3$ begins to precipitate at pH = 4 and dissolves at pH = 9, whereas $Zr(OH)_4$ begins to precipitate at pH = 2 and does not dissolve in a basic medium; (ii) because of the claim[18] that the precipitation of hydrous zirconia in a basic medium produces a precursor that can be converted into ZrO_2 with a surface area higher than that obtainable at lower pH.

Table 1 reports analytical and morphological data relative to all samples calcined at 923 K. Sulfur content ranges between 2.3 and 3.5 SO_4 groups/nm^2, i.e., somewhat below the figure of 4 SO_4 groups/nm^2, corresponding to the value estimated for a full (statistical) monolayer.[19] The addition of Al_2O_3 increases the specific surface area by some 30% in comparison with plain ZS, but BET values do not change significantly with the Al_2O_3 amount added.

The complete N_2 adsorption−desorption isotherms of all samples, regardless of the amount of alumina added, are type IV (BDDT classification[20]) and are characteristic of well-developed mesoporous systems. The isotherms of three representative samples are shown in Figure 1.

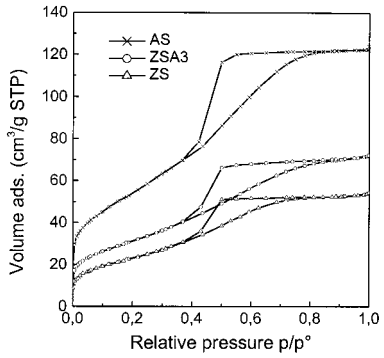

Figure 1. Nitrogen adsorption hysotherms for ZS, ZSA3, and AS catalysts.

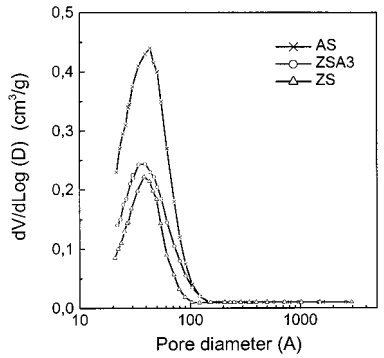

Figure 2. BJH mesopore distribution for ZS, ZSA3, and AS catalysts.

The shape of the hysteresis loop is type H2, according to IUPAC classification:[21] this type of loop is typical of solids consisting of particles crossed by nearly cylindrical channels or constituted by aggregates (consolidated) or agglomerates (unconsolidated) of spheroidal particles.[22] Pores usually have nonuniform size or shape. Hysteresis is usually attributed to a different size of pore mouth and pore body or to a different behavior in adsorption and desorption in near cylindrical pores.

The total pore volume (V_p), calculated from the plateau of the corresponding adsorption isotherms, shows a trend similar to that of the BET surface area.

The mesopore size distribution for each sample was obtained from the adsorption branch of the isotherms, following the BJH procedure.[12,23] For H2 type isotherms, the desorption of nitrogen is limited by the narrow neck of the pore, and information about the body of the pore can only be obtained from the analysis of the adsorption isotherm branch.[24,25] The pore size distribution of three representative samples is shown in Figure 2: all the samples exhibit a unimodal pore size distribution with the most frequent pore diameter of ≈40 Å.

The effect of alumina content on the catalytic activity of a sulfated zirconia system was studied in *n*-butane

(18) Chuah, G. K.; Jaenicke, S.; Cheong, S. A.; Chan, K. S. *Appl. Catal. A* **1996**, *145*, 267.
(19) Waqif, M.; Bachelier, J.; Saur, O.; Lavalley, J. C. *J. Mol. Catal.* **1992**, *72*, 127.
(20) Brunauer, S.; Deming, L. S.; Deming, W. S.; Teller, E. *J. Am. Chem. Soc.* **1940**, *62*, 1723.
(21) Sing, K. S. W.; Everett, D. H.; Haul, R. A. W.; Moscou, L.; Pierotti, R. A.; Rouquerol, J.; Siemieniewska, T. *Pure Appl. Chem.* **1985**, *57*, 603.
(22) Lecloux, A. J. *Catalysis (Science and Technology)*; Anderson, J. R., Boudard, M., Eds.; Springer-Verlag; Berlin, 1981; p 171.
(23) Barret, E. P.; Joiyner, L. G.; Halenda, P. P. *J. Am. Chem. Soc.* **1951**, *73*, 373.
(24) Chuah, G. K.; Jaenicke, S.; Pong, B. K. *J. Catal.* **1998**, *175*, 80.
(25) Conner, W. C.; Christensen, S.; Topsoe, H.; Ferrero, M.; Pullen, A. *Characterization of Porous Solids II*; Roquerol, J., Rodriguez Reinoso, F., Sing, K. S. W., Ungerl, K. K., Eds.; Elsevier: Amsterdam, 1994; p 151.

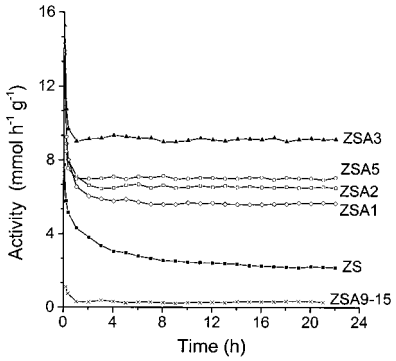

Figure 3. Profile of activity versus time on stream in *n*-butane isomerization.

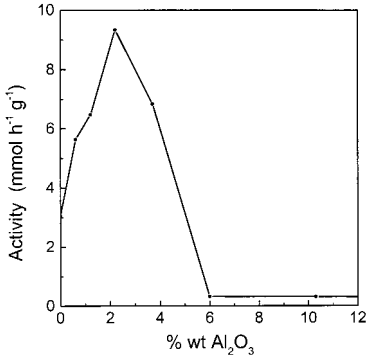

Figure 4. Steady-state isomerization activity as a function of Al_2O_3 amount.

isomerization. This reaction was carried out at 523 K by feeding *n*-butane and H_2 with a ratio 1:4. The selectivity to isobutane was higher than 95% with only minor amounts of propane and methane. The profile of activity versus time on stream is shown in Figure 3. For all catalysts, after a rapid initial decrease of activity, the conversion stabilizes and no deactivation was observed after about 20 h. The initial activity can be completely restored by thermal treatment in air at 723 K. The value of steady state activity was greatly dependent on the alumina amount (Figure 4): a promoting effect is evident only if the Al_2O_3 content is lower than about 5%. If the Al_2O_3 amount increases over this value, the catalytic performance of the promoted catalyst was similar or worse than that of bare sulfated zirconia. Sulfated alumina without zirconia was totally inactive. The maximum steady-state activity (9.3 mmol g^{-1} h^{-1}) was obtained with ZSA3 containing 2.2% of Al_2O_3. Under identical conditions unpromoted sulfated zirconia reached only an activity of 3 mmol g^{-1} h^{-1}. Our results confirm the trend observed by Gao et al.[7] These authors studied the catalytic behavior of Al_2O_3-promoted sulfated zirconia prepared in a similar way and performed the *n*-butane isomerization at the same temperature (523 K) but with a higher ratio H_2/C_4H_{10}, 10/1 instead of 4/1.

The acidity of alumina-promoted sulfated zirconia samples was tested by pyridine adsorption/desorption at room temperature. Before measurement the catalysts were activated in a vacuum at 673 K to simulate the activation pretreatment of the catalytic test. It is well-known that, on oxidic systems, py adsorption at mild temperatures can distinguish between Lewis and Brønsed acidity, at least in qualitative terms. Among the several adsorption bands formed, two absorption bands are easily used to identify the Brønsted and Lewis acidic sites: the analytical band for py−L species at ≈1440 cm^{-1} and the analytical band for py−B species at ≈1545 cm^{-1}. By means of the Lambert−Beer's equation and through the knowledge of the extinction coefficient of these species,[26] it was possible to give a quantitative meaning to the L/B ratio. The results obtained are reported in the last column of the Table 1. The effect of alumina content on the Lewis to Brønsted ratio is evident and the maximun value is reached for SZA3, the catalyst more active in *n*-butane isomerization.

The X-ray diffraction patterns give evidence that the samples ZSA9 and ZSA15, containing 6.0% of Al_2O_3 or more, are completely amorphous, whereas the samples with a lower Al_2O_3 content (i.e., from ZSA1 to ZSA5) as well as the plain sulfated zirconia system (ZS) are semicrystalline. No peaks of any Al_2O_3 crystalline phase were ever observed in the diffractograms, as all crystalline peaks are due only to ZrO_2 phases.

It is well-known[27] that pure ZrO_2 is monoclinic from room temperature up to 1443 K, tetragonal between 1443 and 2653 K,[28] and cubic up to the melting point 2953 K.[29] At ambient temperature the cubic and the tetragonal polymorphs can be stabilized by forming solid solutions with oxides such as Y_2O_3, CaO, and Yb_2O_3.[30−32] The tetragonal form (t-ZrO_2) has been reported to be stabilized also by small size crystallites[33] and the critical size for the stabilization has been estimated to be ≈300 Å.

In their characterization of alumina-containing sulfated zirconia, Zalewsky et al.[10] claimed that the effect of alumina was to prevent the formation of large crystallites, thus stabilizing the tetragonal phase.

To understand the structural and microstructural effect of the alumina on the formation and stabilization of the zirconia phases, it is important to follow the behavior and evolution of the amorphous and crystalline phases depending on the alumina loading in the samples. Looking at the X-ray patterns from ZSA1 to ZSA9 (Figure 5a−d), it is possible to note that increasing the alumina loading corresponds to an increment of the amorphous phase formed.

However, there are some basic questions to be answered: (i) the possibility that some of the zirconia remains amorphous together with the alumina; (ii) the possibility that the alumina loading could influence the amount of the amorphous ZrO_2. To answer these questions a modified version of the Rietveld method[14,15] has been used, which allows the separation and the quantification of amorphous and crystalline phases. This can be done without using any internal standard, if either the chemical composition of the amorphous phase or the global sample composition is known. Because the alumina quantity is known and from the Rietveld analysis we obtain the quantities of crystalline zirconia phases,

(26) Emeis, C. A. *J. Catal.* **1993**, *141*, 347.
(27) Smith, D. K.; Newkirk, H. W. *Acta Crystallogr.* **1965**, *18*, 983.
(28) Teufer, G. *Acta Crystallogr.* **1962**, *15*, 1187.
(29) Aldebert, P.; Traverse, J.-P. *J. Am. Ceram. Soc.* **1985**, *68*, 34.
(30) Morinaga, M.; Cohen, J. B.; Faber, J., Jr. *Acta Crystallogr.* **1979**, *A35*, 789.
(31) Steele, D.; Fender, B. E. F. *J. Phys. C.: Solid State Phys.* **1974**, *7*, 1.
(32) Tien, T. Y.; Subbarao, E. C. *J. Chem. Phys.* **1963**, *39*, 1041.
(33) Garvie, R. C. *J. Phys. Chem.* **1965**, *69*, 1238.

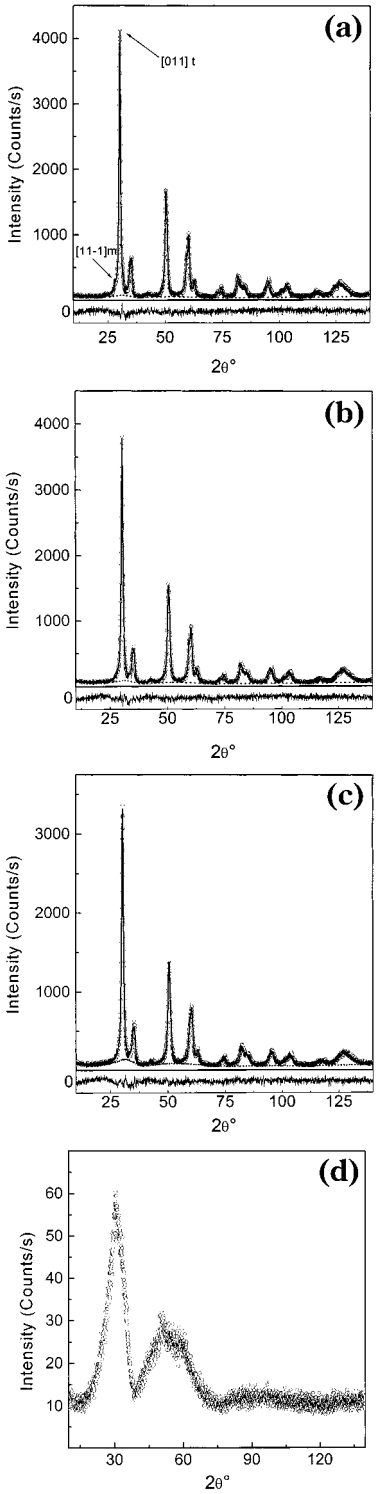

Figure 5. (a) Rietveld analysis of sample ZSA1. The dotted line represents the total amorphous phase. The weighted residuals[14] are reported at the bottom. (b) As in Figure 5 (a) but for sample ZSA3. (c) As in Figure 5 (a) but for sample ZSA5. (d) X-ray diffraction pattern of sample ZSA9.

we can determine the unknown quantity of amorphous zirconia possibly present in our samples. The results obtained from the Rietveld quantitative analysis are reported in Table 2. The Rietveld analysis shows that zirconia crystallizes both in the monoclinic and in the tetragonal form in the samples containing 0% (ZS) and 0.6% (ZSA1) of Al_2O_3, whereas no monoclinic zirconia is present any longer in the samples with higher Al_2O_3 content. Line-broadening analysis was carried out according to a previously described procedure,[34] which combines the results obtained by the Rietveld method and Fourier analysis: the optimized parameters concerning the peaks relevant to the $K\alpha_1$ monochromatic radiation was analytically Fourier transformed and deconvoluted from the instrumental broadening. The minimum crystallite dimension detectable with X-ray wide angle scattering is about 1.5 nm. The crystallite dimensions are reported in Table 2.

Confirmation of some of the results obtained from X-ray diffraction studies has been obtained by Raman measurements. In fact, the Raman spectra in the region below 800 cm^{-1} (Figure 6) clearly indicate that the t-ZrO_2 form is only present in samples containing less than 6.0% Al_2O_3 (ZSA9): the spectra of the latter sample (Figure 6c) and of the ZSA15 sample (not reported here for sake of brevity) show only a broad and nonresolved band, which is consistent with the presence of an amorphous phase.

In more detail, Figure 6a reports the spectrum of the plain ZS sample. Bands at 148, 268, 319, 461, and 648 cm^{-1}, characteristic of tetragonal zirconia,[35−38] are clearly recognized. Minor frequency differences with respect to the spectra reported in the literature are probably a consequence of the preparation of the tetragonal phase, whose stabilization at ambient temperature is due to the presence of surface sulfates. Figure 6b shows the spectrum of ZSA5. In this case, the main spectral features of the tetragonal phase can still be recognized, although the bands are far less intense and much broader than in the previous case, indicating the presence of disorder. Different is the situation that can be observed in the spectrum of ZSA9 (Figure 6c): the bands of the tetragonal phase cannot be observed any longer, whereas a new broad band, centered at about 400 cm^{-1} but extending up to 600 cm^{-1}, appears. By comparison with what is reported in the literature,[37] the latter almost featureless band can be interpreted as due to an amorphous phase. It is in any case clear that the spectrum of Figure 6c cannot be ascribed to the cubic zirconia phase, as the latter presents a well-defined band at ≈600 cm^{-1}.[39] The spectrum of the ZSA15 specimen does not show any new features with respect to that of ZSA9.

Finally, the systems of interest have been characterized from the morphological point of view by the use of electron microscopy (HRTEM). Some of the relevant data are presented in Figure 7. The image in Figure 7a is relative to the parent ZS system. Rather irregular-shaped crystallites of some 8−10-nm average size dominate and exhibit sharp interference fringe patterns that monitor a relatively high crystalline order. The spacing distances most frequently observed are (i) primarily, ∼2.64 and ∼2.96 Å, ascribable to the tetrago-

(34) Benedetti, A.; Fagherazzi, A.; Enzo, G.; Battagliarin, S. M. *J. Appl. Crystallogr.* **1988**, *21*, 543.
(35) Perry, C. H.; Lu, F.; Liu, D. W.; Alzyab, B. *J. Raman Spectrosc.* **1990**, *21*, 577.
(36) Sekulic, A.; Furic, A.; Tonejc, A.; Tonejic, A. M.; Stubicar, M. *J. Mater. Sci. Lett.* **1997**, *16*, 260.
(37) Keramidas, G.; White, W. B. *J. Am. Ceram. Soc.* **1974**, *57*, 22.
(38) Fagherazzi, G.; Canton, P.; Benedetti, A.; Pinna, F.; Mariotto, G.; Zanghellini, E. *J. Mater. Res.* **1997**, *12*, 318.
(39) Cai, J.; Raptis, C.; Raptis, Y. S.; Anastassakis, E. *Phys. Rev.* **1995**, *B 51*, 201.

Table 2. Determination of the Amount of Amorphous and Crystalline (Tetragonal and Monoclinic) Phases by X-ray Diffraction Analysis

		ZrO_2					
sample	Al_2O_3 (wt %)	monoclinic (wt %)	tetragonal (wt %)	amorphous (wt %)	total amorphous (wt %)	$\langle D\rangle$m (Å)	$\langle D\rangle$t (Å)
ZS	0.0	16.5	81.1	2.4	2.4	90	95
ZSA1	0.6	4.2	85.8	9.4	10.0	60	82
ZSA2	1.2		91.7	7.1	8.3		80
ZSA3	2.2		91.2	6.6	8.8		73
ZSA5	3.7		77.2	19.0	22.8		67
ZSA9	6.0				100		
ZSA15	10.3				100		
AS	100.0				100		

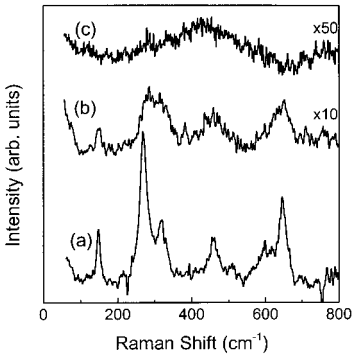

Figure 6. Raman spectra of powders of ZS (a), ZSA5 (b), and ZSA9 (c) with an exciting laser line at 488 nm.

nal phase of zirconia (the (002) and (111) crystal planes, respectively) and (ii) to a lower extent, ~2.84 Å, ascribable to the monoclinic phase of zirconia (the (111) crystal planes). The image in Figure 7b, relative to the sample ZSA3, indicates that when Al_2O_3 is added to the sulfated zirconia system with a loading up to 2.2%, the morphological features of the oxidic system are very little affected by the presence of the additive. The major morphological difference consists of a smaller average size of the crystallites (5−8 nm), which present also more roundish edges, indicative of a more defective termination. The crystallites are very thin, as confirmed by the ability of inspecting overlapping particles and by the presence of typical Moiré fringes (generated by the superimposition of crystallites possessing equal or very similar spacing distances). The crystalline order is always quite high, and a somewhat less sharp resolution of the particles contours is mainly ascribable to the smaller size. As for the crystal phases present and the relevant termination, the still well-resolved interference fringe patterns confirm the assignment to the same low-index planes of the tetragonal ZrO_2 phase reported above for the parent ZS material, but no interference fringes ascribable to the monoclinic ZrO_2 phase can be evidenced anymore. It is thus confirmed what is suggested by other techniques: the addition of small amounts of alumina stabilizes the tetragonal zirconia phase to the point that this is the only phase present.

When alumina is added in percentages higher than 2.2%, the morphological features of the particles become more and more modified. In particular, the contours become more and more roundish, and the possibility of resolving regular fringe patterns is gradually lost (Figure 7c: ZSA5). When the quantity of the additive reaches 6.0% (ZSA9), the system appears as completely amorphous. As an example, the image in Figure 7d reports the features of the sample ZSA15 (10.3%): the average size of the particles is still of the order of some 5−8 nm, but no interference fringes are observable anymore and a thick amorphous overlayer seems to coat the particles. These microscopic data are consistent with a virtually constant surface area of ZSA systems, and with the gradual loss of crystalline order in ZSA systems characterized by a high content of alumina.

4. Discussion

From the data reported it is evident that the sample containing 2.2% of Al_2O_3 (ZSA3) has the highest value of all the parameters considered: it is the most catalytically active, has the highest SO_4 content, has the highest $ZrO_2^{tetragonal}/ZrO_2^{amorphous}$ ratio, and has the highest Lewis to Brønsted acid sites ratio. The strongest ZSA3 catalytic activity could be due to these different factors acting together. In fact, both samples containing monoclinic zirconia (ZS, ZSA1) and the sample ZSA5 containing a higher percentage of amorphous zirconia and less tetragonal phase are not very active. Furthermore, it is important to note that the sample ZSA2 has a very high quantity of tetragonal phase but the SO_4 content and the L/B ratio are not as high as those in the ZSA3 and ZSA2's catalytic activity is lower than ZSA3's.

The fact that the ZSA3 is richer in SO_4 content than ZSA2, despite a similar quantity of tetragonal phase, analogous crystallite dimensions and surface area could be explained considering the different quantity of Al_2O_3 present. It is well-known that Al_2O_3 bonds SO_4 more strongly than ZrO_2 so the higher alumina content in ZSA3 could help in stablizing the bonding of sulfate groups.[19] The effect of the sulfate species seems to enhance the number of Lewis acid sites with respect to the number of Brønsted sites.

To investigate if the promotion was a simple additive effect, we prepared two mechanical mixtures, both containing 3 mol % of Al_2O_3. The first was obtained by adding ZS to AS both calcined at 923 K, the second by mixing the two sulfated hydroxides dried at 383 K, and then calcinating this mixture at 923 K. When submitted to the same reaction conditions, the two mixtures showed the same profile of conversion of unpromoted sulfated zirconia catalyst. It follows that the alumina promotion on zirconia is not due to a simple additive effect and develops before the calcination step. This result is only partially in agreement with the report of Zalewski et al.[10] They also claimed that enhanced catalytic activity is not observed if sulfated zirconia and commercial alumina are mixed after calcination. On the other hand, they observed catalytic improvement with

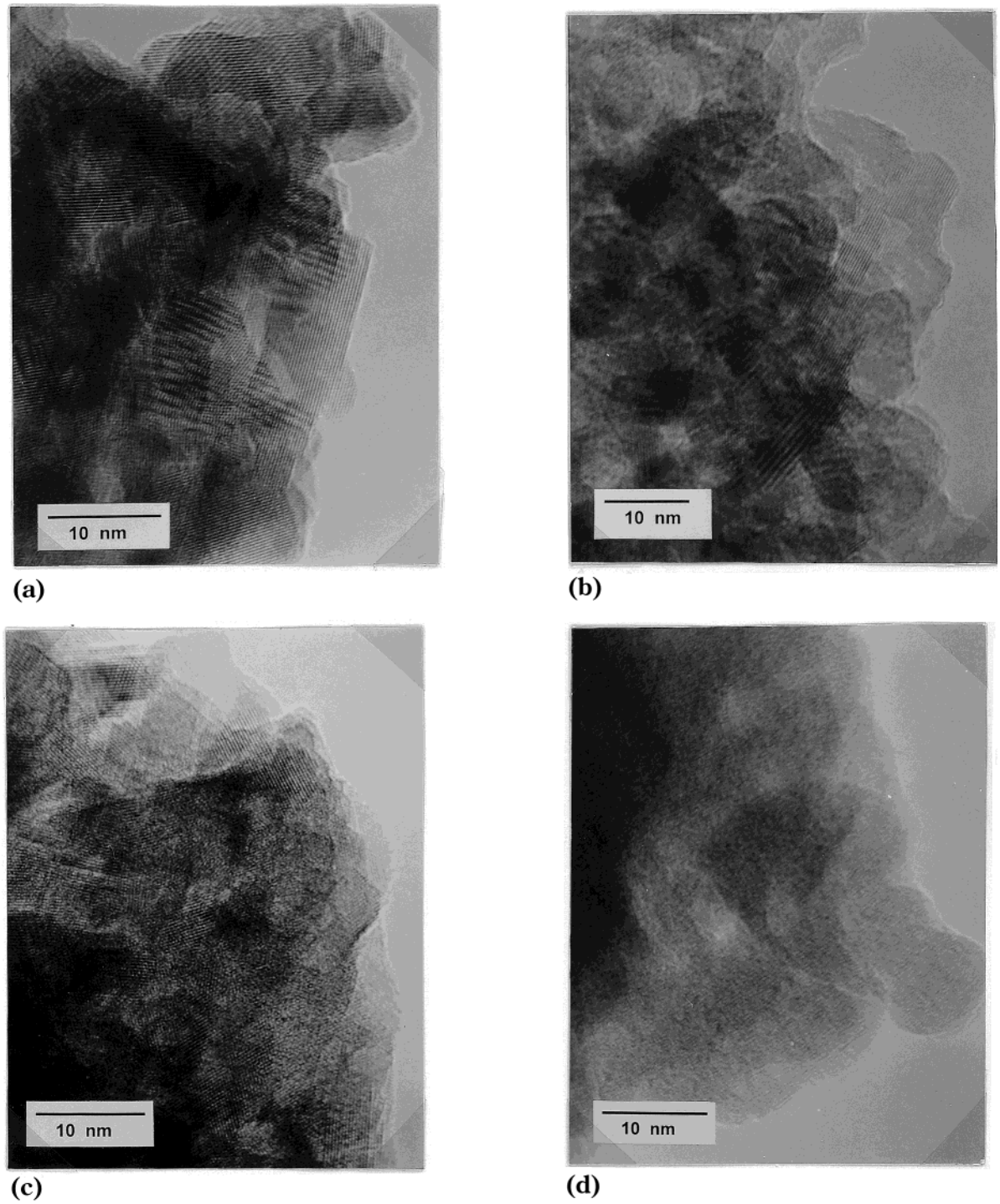

Figure 7. HR-TEM images of ZS (a), ZSA3 (b), ZSA5 (c), and ZSA15 (d) samples.

the sample obtained by calcination of the mixture of sulfated zirconium hydroxide and commercial alumina, both amorphous. It is most likely that the different procedures used for catalyst preparation determined the activity differences found in these two works. We dry-mixed the two amorphous sulfated hydroxides while Zalewski et al.,[10] as far we could understand, obtained their sample by mixing uncalcined sulfated zirconium hydroxide with a commercial unsulfated alumina hydroxide in distilled water.

From the results obtained, it is evident that the Al_2O_3 has also a dramatic effect on the growth of ZrO_2 crystallites: the higher the alumina content, the smaller the crystallite dimensions, so that the tetragonal form is stabilized with respect to the monoclinic one. For an alumina content higher than 3.7% (ZSA9, ZSA15), it is not possible to distinguish any crystalline peaks and only very broad halos are present.

The Al_2O_3 content seems so to influence also the amount of amorphous phase. In fact, the plain sulfated zirconia (ZS sample) is almost completely crystalline (97.6%), but the introduction of a small amount of alumina (i.e., less than 1%) brings about an increase of the amorphous phase from 2.4% (ZS) to 10% (ZSA1). The effect of alumina content on the growing process of zirconia crystallites could be understood by looking at the quantity of zirconia remaining in the amorphous phase. From the quantitative analysis it is possible to

note that the addition of a very small amount of Al_2O_3 (0.6%, ZSA1) gives rise to (i) a drastic decrease of the monoclinic phase, (ii) a little increase of the tetragonal phase, and (iii) the formation of 9.4% of ZrO_2 amorphous phase.

The addition of a quantity of Al_2O_3 as small as 1.2% (ZSA2) is able to inhibit completely the formation of the monoclinic phase and to increase the formation of the tetragonal phase instead of the amorphous one. This behavior is enhanced in the sample containing 2.2% of Al_2O_3 (ZSA3): in this case the ratio $ZrO_2^{(tetragonal)}/ZrO_2^{(amorphous)}$ is even larger than that of the previous ZSA2 sample. The addition of 3.7% of Al_2O_3 (ZSA5) results in a dramatic increase of the amorphous zirconia moiety (19%) and in a decrease of the crystallite dimensions. In fact, for the tetragonal phase the average dimension changes from a starting value of 95 Å in the ZS sample to a value of 67 Å for the ZSA5 sample.

The alumina could act as a filler among the zirconia crystallites, thus preventing their growth, or it could deposit on the surface of the zirconia particles. In both cases the effect is to prevent the diffusion of the zirconia particles and their sintering. The second hypothesis of the covering of zirconia by alumina is supported by the TEM results that show that for the increase in the alumina content, the particles are coated more and more by an amorphous overlayer. The covering of the zirconia particles by the amorphous moiety could hinder the active sites, thus reducing the catalytic activity for samples with a higher alumina content.

4 Conclusions

The influence of the addition of small amounts of Al_2O_3 on the structure and microstructure of ZrO_2 has been reported.

The use of the modified version of the Rietveld analysis has allowed us to follow the changes in the amorphous and crystalline phase composition with the different amounts of alumina and to quantify the wt % composition of the present phases. The analysis has evidenced the following:

(i) No peaks of any Al_2O_3 crystalline phase were ever observed in the diffractograms, as all crystalline peaks are due only to ZrO_2 phases.

(ii) No monoclinic zirconia is present any longer in the samples with an Al_2O_3 content higher than 0.6 wt %.

(iii) The Al_2O_3 content influences the growth of zirconia crystallites: the higher the alumina content, the smaller the crystallite dimensions, so that the tetragonal form is stabilized with respect to the monoclinic one.

(iv) The Al_2O_3 content seems to influence also the amount of amorphous phase: the introduction of a small alumina amount (i.e., less than 1 wt %) brings about an increase of the amorphous phase from 2.4 to 10 wt %.

These results have been confirmed also by TEM and Raman measurements.

The addition of Al_2O_3 increases the specific surface area by some 30% in comparison with plain ZS, but BET values do not change significantly with the Al_2O_3 amount added.

Acknowledgment. The financial support from MURST (Project COFIN-98) is gratefully acknowledged.

CM001101Z